16

Silicon Carbide: Synthesis and Properties

Houyem Abderrazak[1] and Emna Selmane Bel Hadj Hmida[2]
[1] *Institut National de Recherche et d'Analyse Physico-Chimique, Pole Technologique Sidi Thabet, 2020, Tunisia*
[2] *Institut Préparatoire Aux Etudes d'Ingénieurs El Manar 2092, Tunisia*

1. Introduction

Silicon carbide is an important non-oxide ceramic which has diverse industrial applications. In fact, it has exclusive properties such as high hardness and strength, chemical and thermal stability, high melting point, oxidation resistance, high erosion resistance, etc. All of these qualities make SiC a perfect candidate for high power, high temperature electronic devices as well as abrasion and cutting applications. Quite a lot of works were reported on SiC synthesis since the manufacturing process initiated by Acheson in 1892. In this chapter, a brief summary is given for the different SiC crystal structures and the most common encountered polytypes will be cited. We focus then on the various fabrication routes of SiC starting from the traditional Acheson process which led to a large extent into commercialization of silicon carbide. This process is based on a conventional carbothermal reduction method for the synthesis of SiC powders. Nevertheless, this process involves numerous steps, has an excessive demand for energy and provides rather poor quality materials. Several alternative methods have been previously reported for the SiC production. An overview of the most common used methods for SiC elaboration such as physical vapour deposition (PVT), chemical vapour deposition (CVD), sol-gel, liquid phase sintering (LPS) or mechanical alloying (MA) will be detailed. The resulting mechanical, structural and electrical properties of the fabricated SiC will be discussed as a function of the synthesis methods.

2. SiC structures

More than 200 SiC polytypes have been found up to date (Pensl, Choyke, 1993). Many authors proved that these polytypes were dependent on the seed orientation. For a long time, (Stein et al, 1992; Stein, Lanig, 1993) had attributed this phenomenon to the different surface energies of Si and C faces which influenced the formation of different polytypes nuclei. A listing of the most common polytypes includes 3C, 2H, 4H, 6H, 8H, 9R, 10H, 14H, 15R,19R, 2OH, 21H, and 24R, where (C), (H) and (R) are the three basic cubic, hexagonal and rhombohedral crystallographic categories. In the cubic zinc-blende structure, labelled as 3C-SiC or β-SiC, Si and C occupy ordered sites in a diamond framework. In hexagonal polytypes *n*H-SiC and rhombohedral polytypes *n*R-SiC, generally referred to as α-SiC, *n*Si-C bilayers consisting of C and Si layers stack in the primitive unit cell (Muranaka et al, 2008).

SiC polytypes are differentiated by the stacking sequence of each tetrahedrally bonded Si-C bilayer. In fact the distinct polytypes differ in both band gap energies and electronic properties. So the band gap varies with the polytype from 2.3 eV for 3C-SiC to over 3.0 eV for 6H-SiC to 3.2 eV for 4H-SiC. Due to its smaller band gap, 3C-SiC has many advantages compared to the other polytypes, that permits inversion at lower electric field strength. Moreover, the electron Hall mobility is isotropic and higher compared to those of 4H and 6H-polytypes (Polychroniadis et al, 2004). Alpha silicon carbide (α-SiC) is the most commonly encountered polymorph; it is the stable form at elevated temperature as high as 1700°C and has a hexagonal crystal structure (similar to Wurtzite). Among all the hexagonal structures, 6H-SiC and 4H-SiC are the only SiC polytypes currently available in bulk wafer form.
The β-SiC (3C-SiC) with a zinc blende crystal structure (similar to diamond), is formed at temperatures below 1700°C (Muranaka et al, 2008). The number 3 refers to the number of layers needed for periodicity. 3C-SiC possesses the smallest band gap (~2.4eV) (Humphreys et al,1981), and one of the largest electron mobilities (~800 $cm^2V^{-1}s^{-1}$) in low-doped material (Tachibana et al, 1990) of all the known SiC polytypes. It is not currently available in bulk form, despite bulk growth of 3C-SiC having been demonstrated in a research environment (Shields et al 1994). Nevertheless, the beta form has relatively few commercial uses, although there is now increasing interest in its use as a support for heterogeneous catalysts, owing to its higher surface area compared to the alpha form.

3. Opto-electronic properties of SiC

Silicon carbide has been known since 1991 as a wide band gap semiconductor and as a material well-suited for high temperature operation, high-power, and/or high-radiation conditions in which conventional semiconductors like silicon (Si) cannot perform adequately or reliably (Barrett et al, 1991). Additionally, SiC exhibits a high thermal conductivity (about 3.3 times that of Si at 300 K for 6H-SiC) (Barrett et al, 1993). Moreover it possesses high breakdown electric-field strength about 10 times that of Si for the polytype 6H-SiC.
In table 1, a comparison of fundamental properties of the main encountered SiC polytypes with the conventional Si semiconductor is depicted (Casady, Johonson, 1996).

Quantity	3C-SiC	4H-SiC	6H-SiC	Silicon
Thermal conductivity ($W\ cm^{-1}K^{-1}$) at 300K doped at ~$10^{17}cm^{-3}$	3.2	3.7	4.9	1.5
Intrinsic carrier concentration at 300K (cm^{-3})	$1.5x10^{-1}$	$5x10^{-9}$	$1.6x10^{-6}$	$1.0x10^{10}$
Saturation velocity ($cm\ s^{-1}$) parallel to c-axis	-	$2.0x10^7$	$2.0x10^7$	$1.0x10^7$
Electron mobility ($cm^2V^{-1}s^{-1}$)	800	1000	400	1400
Hole mobility ($cm^2V^{-1}\ s^{-1}$)	40	115	101	471
Schottky structures ε_s	9.72		9.66	11.7

Table 1. Comparison of some silicon carbide polytypes and silicon material properties (Casady, Johonson, 1996)

However, SiC possesses a much higher thermal conductivity than the semi-conductor GaAs at a temperature as high as 300 K as well as a band gap of approximately twice the band gap of GaAs. Moreover, it has a saturation velocity (v_{sat}) at high electric fields which is superior to that of GaAs and a saturated carrier velocity equal to GaAs at the high field power (Barrett et al, 1993).
The band gap of Si, GaAs and of 6H-SiC are about to 1.1 eV, 1.4 eV and 2.86 respectively.
We found a compilation of properties of: Silicon, GaAs, 3C-SiC (cubic) and 6H-SiC (alpha) with repeating hexagonal stacking order every 6 layers. SiC has a unique combination of electronic and physical properties which have been recognized for several decades (O'Connor, Smiltens, 1960).
In the following table a comparison of several important semiconductor material properties is given (Han et al, 2003).

Properties	Si	GaAs	3C-SiC	6H-SiC	4H-SiC
Band gap (eV) (T<5K)	1.12	1.43	2.40	3.02	3.26
Saturated electron drift velocity (10^7 cm s^{-1})	1.0	2.0	2.5	2.0	2.0
Breakdown field (MV cm^{-1})	0.25	0.3	2.12	2.5	2.2
Thermal conductivity (W cm^{-1} K^{-1})	1.5	0.5	3.2	4.9	3.7
Dielectric constant	11.8	12.8	9.7	9.7	9.7
Physical stability	Good	Fair	Excellent	Excellent	Excellent

Table 2. Comparison of several important semiconductor material properties (Han et al, 2003).

Silicon carbide also has a good match of chemical, mechanical and thermal properties. It demonstrates high chemical inertness, making it more suitable for use in sensor applications where the operating environments are chemically harsh (Noh et al, 2007).

4. Methods to grow SiC single crystals

Naturally silicon carbide occurs as moissanite and is found merely in very little quantities in certain types of meteorites. The most encountered SiC material is thus man made. Traditionally, SiC material has been produced through the Acheson process, in an Acheson graphite electric resistance furnace, which is still used for production of poly-crystalline SiC that is suitable for grinding and cutting applications.
In this process a solid-state reaction between silica sand and petroleum coke at very high temperature (more than 2500°C) leads to the formation of silicon carbide under the general reaction (1) (Fend, 2004):

$$SiO_2(s) + 3C(s) \longrightarrow SiC(s) + 2CO(g) \quad (1)$$

Crystalline SiC obtained by the Acheson-Process occurs in different polytypes and varies in purity. In fact during the heating process and according to the distance from the graphite resistor heat source of the Acheson furnace, different coloured products could be formed. Thus, colourless, transparent or variously coloured SiC materials could be found (Schwetk et al, 2003). Additionally, the manufactured product has a large grain size and is invariably contaminated with oxygen. Moreover Nitrogen and aluminium are common impurities, and they affect the electrical conductivity of SiC. Thus the as, obtained SiC ceramic, often known by the trademark carborundum, is adequate for use as abrasive and cutting tools.
The conventional carbothermal reduction method for the synthesis of SiC powders is an excessive demanding energy process and leads to a rather poor quality material. Several alternative methods have been reported in the literature for the synthesis of pure SiC.

4.1 Physical vapor transport (PVT)

Physical vapor transport (PVT), also known as the seeded sublimation growth, has been the most popular and successful method to grow large sized SiC single crystals (Augustin et al, 2000; Semmelroth et al 2004). The first method of sublimation technique, known as the Lely method (Lely, Keram, 1955) was carried out in argon ambient at about 2500°C in a graphite container, leading to a limited SiC crystal size. Nevertheless, although the Lely platelets presented good quality (micropipe densities of 1-3 cm^{-2} and dislocation densities of 10^2-10^3 cm^{-2}), this technique has presented major drawbacks which are the uncontrollable nucleation and dendrite-like growth.
Given the fact that the control of SiC growth by the PVT method is difficult and the adjustment of the gas phase composition between C and Si complements and/or dopant species concentration is also limited, (Tairov, Tsvetkov, 1978) have developed a modified-Lelly method also called physical vapor transport method or seed sublimation method. In fact, this latter was perfected by placing the source and the seed of SiC in close proximity to each other, where a gradient of temperature was established making possible the transport of the material vapor in the seed at a low argon pressure.
The conventional PVT method has been refined by (Straubinger et al, 2002) through a gas pipe conveying between the source and the crucible into the growth chamber (M-PVT setup). Considering this new approach, high quality 4H and 6H-SiC, for wafer diameters up to 100 mm, were grow. In addition 15R-SiC and 3C-SiC were also developed.
to control the gas phase composition, (Wellmann et al, 2005) have developed the conventional configuration by the Modified PVT technique (M-PVT) for preparation of SiC crystal. They have also, using an additional gas pipe for introduction of doping gases and/or small amounts of C- and Si- containing gases (silane: SiH_4:H_2-1:10 and propane: C_3H_8).

$v = 10v_0$	$v = 5v_0$	$v = v_0$
No growth	Growth observed	The quality of crystal growth was found improved to the conventional setup configuration without a gas pipe.

v_0 and v are the PVT and the gas fluxes, respectively.
Table 3. The impact of the gas fluxes on the crystal growth.

The modified PVT system showed the improvement of the conventional PVT system of SiC. In fact, (Wellmann et al, 2005) have demonstrated that small additional gas fluxes in the

modified- PVT configuration have a stabilizing effect on the gas flow in the growth cell interior compared to the conditional PVT configuration without the gas pipe. Table 3 shows the impact of the gas fluxes on the SiC crystal growth.
In the case of doping, using nitrogen as n-type doping, the gas was supplied directly in front of the growth interface so this modified growth presented an advantage for the high purity doping source. Phosphorus has been either used as n-type doping because it has a higher solid solubility (10 times higher than the state-of-the-art donor nitrogen) (M. Laube et al, 2002) and (Wellmann et al, 2005) have achieved phosphorus incorporation of approximately $2x10^{17}cm^{-3}$ but this hasn't reached the kinetic limitation value.
In contrast, aluminum has been used for p-type doping, the axial aluminum incorporation was improved, the conductivity reached 0.2 $\Omega^{-1}cm^{-1}$ in aluminum doped 4H-SiC which meets the requirement for bipolar high-power devices.
However, many factors can influence the crystal polytype. (Li et al, 2007) reported the effect of the seed (root-mean-square: RMS) on the crystal polytype. (Stein et al, 1992; Stein, Lanig, 1993) attributed this phenomenon for a long time to the different surface energies of Si and C faces which influenced the formation of different polytypes nuclei. In this case the sublimation of physical vapor transport system was used to grow SiC single crystal. In order to do so, the SiC powder with high purity was placed in the bottom of the crucible at the temperature range (2000-2300°C). Whereas the seed wafer was maintained at the top of the graphite crucible at the temperature range (2000-2200°C) in argon atmosphere and the pressure in the reaction chamber was kept at 1000-4000 Pa. After about ten hours of growth, three crystal slices of yellow, mixed (yellow and green) and green zone were obtained.
According to (Li et al, 2007), it was found that polytypes are seed RMS roughness dependent. In fact, the crystal color is more and more uniform with the decreasing seed RMS roughness. The yellow coloured zone corresponds to the 4H-SiC polytype, while the green zone is attributed to 6H-SiC and the mixed zones correspond to the mixture of 6H and 4H-SiC polytypes.
The X-Ray direction funder showed that the two zones were grown in different directions (<0001> and $<11\bar{2}0>$ for yellow and green zone respectively).

The following table summarizes the obtained results of the as synthesized crystals:

Properties	A: Yellow Zone 4H-SiC	B: Green zone 6H-SiC	C: Mixed zone of 4H and 6H-SiC
Raman spectra peaks (cm^{-1})	776-767-966	766-788-796-966	766-776-796-788-966
Hall Effect measurement carrier densities ($10^{16}cm^{-3}$)	6.84	0.82	_
X-Ray direction funder	<0001>	$<11\bar{2}0>$	_
The distance values between the two adjacent faces (nm) by HRTEM micrographs	0.253	0.155	_

Table 4. Raman spectra peaks, Hall Effect and HRTEM of A, B and C (Li et al, 2007).

According to (Ohtani et al, 2009), SiC power diodes and transistors are mainly used in high efficiency power system such as DC/AC and DC/DC converters. For these applications, to

obtain a sufficiently low uniform electrical resistivity's and to prevent unnecessary substrate resistance, nitrogen can be easily introduced into the crystals (the growth rates employed were relatively low (0.2-0.5 mm/h)) during physical vapor transport in terms of growth temperature dependence.

4H-SiC crystals were grown on well-and off oriented 4H-SiC $(000\bar{1})$C seed crystals by the PVT growth where the doping resulted in n^+4H-SiC single crystals having bulk resistivities less than 0.01Ωcm.

The resistivity decreased while the nitrogen concentration in SiC crystals increased as the growth temperature was lowered. A 4H-SiC grown at 2125°C exhibited an extremely low bulk resistivity of 0.0015 Ωcm (lowest ever reported). The resistivity change was attributed to the formation of extremely low density of 3C-SiC inclusions and double shockly stacking faults in the substrates. Their presence depended on the surface preparation conditions of substrates then we can say that the primary nucleation sites of the stacking faults exist in the near-surface-damaged layers of substrates.

At low-growth temperatures, nitrogen incorporation was enhanced. This could be attributed to the increased nitrogen coverage of the growing surface at low temperature, or to the low-growth rates resulting from the low-growth temperatures.

On the other hand, authors have showed that the lower growth temperatures cause macrostep formation on the $(000\bar{1})$C facet of heavily nitrogen doped 4H-SiC single crystals.

The crystals showed a relatively sharp X-ray rocking curve even when the crystals were doped with a nitrogen concentration of $5.3x10^{19}$-$1.3x10^{20}$ cm^{-3} and almost no indication of 3C-SiC inclusions or stacking faults was detected in the crystals. It was also shown that the peaks were quite symmetrical suggesting a good crystalinity of the crystal.

4.2 Chemical Vapor Deposition (CVD)

Chemical vapor deposition (CVD) techniques have the largest variability of deposition parameters. The chemical reactions implicated in the exchange of precursor-to-material can include thermolysis, hydrolysis, oxidation, reduction, nitration and carboration, depending on the precursor species used. During this process, when the gaseous species are in proximity to the substrate or the surface itself, they can either adsorb directly on the catalyst particle or on the surface. Thus the diffusion processes as well as the concentration of the adsorbates (supersaturation) leads to a solid phase growth at the catalyst–surface interface. (Barth et al, 2010)

CVD is one of the suitable used methods to produce SiC in various shapes of thin films powders, whiskers and nanorods using Si-C-HCl system. Amorphous fine silicon carbide powders have been prepared by CVD method in the SiH_4-C_2H_2 system under nitrogen as a carrying gas (Kavcký et al, 2000). Reaction (1) was expected to take place in the reaction zone:

$$2\,SiH_{4(g)} + C_2H_{2(g)} \longrightarrow 2SiC\,(g) + 5H_{2(g)} \qquad (2)$$

The influence of the given reaction conditions are summarized in table 5:

Sample no	Temperature (°C)	Ratio C_2H_2:SiH_4	Ratio C:Si	Flow rate (cm^3 min^{-1})	Colour
1	900	1.2:1	2.4:1	130	Brown
2	1100	1.2:1	2.4:1	130	Black
3	1200	1.2:1	2.4:1	130	Black
4	1250	1.2:1	2.4:1	130	Black
5	1100	1.6:1	3.1:1	178	Black
6	1100	0.9:1	1.8:1	163	Brown-Black
7	1100	2.1:1	4.2:1	143	Brown-Black

Table 5. Reaction condition (Kavcký et al, 2000)

The presence of crystallized form of SiC was proven by infrared spectroscopy (IR) and X-ray Diffraction (XRD) investigations. Whereas, chemical analysis did not detect formation of Si_3N_4 under the indicated reaction conditions. (Kavcký et al, 2000).

From the morphology examinations it was revealed that the powder products were related to the C_2H_2:SiH_4 ratio in the initial gas mixture. The temperature of 1100°C was an optimum to C_2H_2:SiH_4 ratio 1.2:1. The particle size of SiC powder was narrow in the range of 0.1-0.5 μm and consists of quasi-spherical particles. In addition the growth increased faster than the nucleation rate with temperature.

(Fu et al 2006) obtained SiC using CH_3SiCl_3 (MTS) and H_2 as precursors by a simple CVD process, without using metallic catalyst, and under atmospheric pressure. Thus, SiC nanowires with high purity and homogenous diameter were formed.

High purity argon gas was fed into the furnace to maintain an inert atmosphere. H_2 gas was used as carrier gas, which transfers MTS through a bubbler to the reactor gas as well as diluent's gas. This latter gas regulates the concentration of the mixture containing MTS vapor and carrier gas. During growth, the furnace was maintained at 1050-1150°C for 2 h under normal atmosphere pressure. The substrates were C/C composites.

The following chemical equations can be written to describe the steps leading to SiC crystals:

$$CH_3SiCl_3 + H_2 \longrightarrow CH_4 + SiCl_2 + HCl \quad (3)$$

$$CH_4 + SiCl_2 \longrightarrow SiC + H_2 \quad (4)$$

For CVD process using CH_3SiCl_3 (MTS) (Fu et al 2006) the obtained micrographs revealed that the nanowires generally display smooth surface and homogenous diameter of about 70 nm. The AEM image of an individual nanowire and its corresponding selected-area electron diffraction (SAED) pattern, indicated a single crystalline structure of the nanowire. The XRD investigations of nanowires revealed diffracting peaks of both graphite and cubical β-SiC corresponding to the substrate and the nanowires.

Authors reported that the width and length of nanowires were primarily controlled by the deposition temperature. At higher deposition temperature, the growth rate of SiC grains became larger and the crystal grains became bigger. In addition, a special structure with an amorphous SiO_2 wrapping layer on the surface of SiC nanowire was also found.

4.3 Sol-gel processing technique for synthesizing SiC

Sol-gel processing received extensive attention in the 1970s and early 1980s as hundreds of researchers sought after novel, low temperature methods of producing common oxide ceramics such as silica, alumina, zirconia and titania in fully dense monolithic form (Brinker et al, 1984).

The basic advantages of using the sol-gel synthesis approach have been the production of high pure product with extremely uniform and disperse microstructures not achievable using conventional processing techniques because of problems associated with volatilization, high melting temperatures, or crystallization. In addition, the production of glasses by the sol-gel method permits preparation of glasses at far lower temperatures than is possible by using conventional melting. Moreover, the sol-gel process has proved to be an effective way for synthesis of nanopowders. Finally, sol-gel approach is adaptable to producing films and fibers as well as bulk pieces.

The composites produced have included both metal-ceramic and ceramic-ceramic materials, some carefully doped with additional phases (easily performed with sol-gel process). It was found that the as obtained materials have exhibited favourable physical and mechanical properties, some of which can be attributed to their synthesis process (Rodeghiero et al, 1998).

The sol-gel process comprises two main steps that are hydrolysis and polycondensation. The first one starts by the preparation of a Silica-glass by mixing an appropriate alkoxide as precursor, with water and a mutual solvent to form a solution. Hydrolysis leads to the formation of silanol groups (SiOH) subsequently condensed to produce siloxane bonds (SiOSi). The silica gel formed by this process leads to a rigid, interconnected three-dimensional network consisting of submicrometer pores and polymeric chains. The basic structure or morphology of the solid phase can range anywhere from discrete colloidal particles to continuous chain-like polymer networks (Klein et al, 1980; Brinker et al, 1982).

After solvent removal, that requires a drying process, a xerogel is obtained accompanied by a significant shrinkage and densification. This phase of processing affects deeply the ultimate microstructure of the final component. Conversely, the network does not shrink when solvent removal occurs under hypercritical (supercritical) conditions, an aerogel is consequently produced, a highly porous and low-density material.

However, for industrial applications, this process is rather expensive, as it requires costly precursors, especially compared to the Acheson classical one, starting from sand and coke. Furthermore it is not practical to handle important liquid quantities of reagents. Additionally, the carbothermal reduction of silica is performed at temperatures around 1600°C.

As a way to improve the interest of sol-gel process, it would be interesting to prepare high reactivity precursors, and then to decrease the silica carbothermal reduction temperature and/or to increase the SiC production yield. One approach to accelerate the carbothermal reduction of silica and to increase the yield was performed by (**A**. Julbe et al, 1990), who obtained crystalline β-SiC, after pyrolysis at about 1580°C with a 3h hold, starting from colloidal silica sol and saccharose ($C_{12}H_{22}O_{ll}$) as silicon and carbon sources respectively. Boric acid (H_3BO_3), soluble in aqueous solutions, was directly introduced in the sol.

The SiC powders had grain size of 100 nm in diameter and were easily sinterable (87% of theoretical density) thanks to boron containing additives resulting in submicron and homogeneous product. Moreover, boric acid added in the original colloidal sols improved

significantly the carbothermal reduction yield as well as the conversion rate and the powder crystallinity.

Another approach to enhance the carbothermal reduction yield for the SiC production consists in increasing the reactivity of the precursors. In this context, and by using also boric acid as additive, (Lj. Čerović et al, 1995) synthesised β-SiC at 1550°C by the reductive heating of gel precursors prepared from silica sol and saccharose or activated carbon as carbon sources. It was proved that for SiC formation when starting from silica and with saccharose being the carbon source, the formation of SiC started hardly at 1300°C and became intensive at 1400°C. In contrast, in the case of gels prepared from activated carbon, the crystallization of β-SiC started at 1400°C and progressed via carbothermal reduction of SiO_2 with a high crystallinity. These differences are due to the close contact between SiO_2 and C molecules obtained only if the gels are prepared using saccharose as carbon source. The same behaviour was also observed by (a White et al, 1987; b White et al, 1987) for SiC powder synthesis starting from organosilicon polymers as silicon and carbon precursors. The molecular intimacy of the SiO_2/C mixture resulted in lower temperatures of synthesis and higher surface areas of the produced SiC powders.

It was also established that even though the synthesis of SiC from gels with activated carbon progressed with greater conversion rate than when using saccharose, the boric acid addition was found to be advantageous.

(V. Raman et al, 1995) synthesizing SiC via the sol-gel process from silicon alkoxides and various carbon sources. Tetraethoxysilane (TEOS), methyltriethoxysilane (MTES) and a mixture of TEOS and MTES were used as silicon precursors whereas, phenolic resin, ethylcellulose, polyacrylonitrile (PAN) and starch were used as carbon sources. After hydrolysis the sol was kept at 40 °C for gelling, ageing and drying. The as obtained gels were then heat treated in order to synthesize silicon carbide by carbothermal reduction of silica, largely a used process at industrial scale for its relatively low coat (Schaffe et al, 1987). It was found that all the products obtained from all the precursors are β-SiC. The colour of the products ranged from light-green to greyish-black depending upon the amount of free carbon in the final product.

Since ceramic nanopowders have demonstrated enhanced or distinctive characteristics as compared to conventional ceramic material, considerable attention was devoted to the synthesis methods for nanoscale particles thanks to their potential for new materials fabrication possessing unique properties (Bouchard et al, 2006).

Among methods used to synthesize ceramic nanoparticles, sol-gel processing is considered to be one of the most common and effective used technique. (V. Raman et al, 1995) for synthesizing β-SiC with crystallite size ranging from 9 to 53 nm. This variation is attributed to the difference in the nature of carbon obtained from the various sources. Whereas, the difference observed with the same carbon source is probably due to Si-C of Si-CH_3 linkage present in MTES which is retained during carbonization and carbothermal reduction.

The materials produced by the sol-gel present rather low density compared to other synthesis methods. Indeed, samples prepared by the sol-gel technique are highly porous in nature due to the evolution of gases during carbonization and carbothermal reduction of gel precursors and thus exhibit lower densities compared with the theoretical value for SiC (3.21g /cm^3). (V. Raman et al, 1995) reported the measured samples densities for different silicon and carbon precursors and they presented a maximum density of 1.86 g /cm^3.

The porosity of these gels is the result of solvents, hydrogen, oxygen and nitrogen loss during the carbonisation of precursors resulting in the formation of porous product (silica and carbon). Table 6 summarizes the characteristics of the obtained SiC materials as a function of the different silicon and carbon sources.

Mixture	Silicon Source	Carbon Source	Colour	Crystallite size (nm)	Density (g/cm^3)
1	TEOS	Phenolic resin	Greyish-black	52.5	1.64
2	MTES	Phenolic resin	Grey	32.6	1.60
3	TEOS + MTES	Phenolic resin	Grey	52.5	1.86
4	TEOS	Ethylcellulose	Light-green	23.3	-
5	MTES	Ethylcellulose	Light-green	9	1.76
6	TEOS	PAN	Greyish-black	< 32.6	1.38
7	TEOS	Starch	Greyish-black	21.3	1.80

Table 6. Properties of SiC prepared by sol-gel process from different silicon and carbon Precursors. (V. Raman et al, 1995)

(J. Li et al, 2000) used two step sol-gel process for the synthesis of SiC precursors. The authors synthesized phenolic resin-SiO_2 hybrid gels by sol-gel technique that was used as silicon source in the presence of hexamethylenetetramine (HMTA) as catalysts.
In the first step for prehydrolysis oxalic acid (OA) was added as catalyst and the ratio OA/TEOS was investigated. OA was considered promoting hydrolysis of TEOS. Moreover it was established that the OA content as well as the prehydrolysis time determined whether gel instead of precipitate could form.
For the second step of the sol-gel process, that is gelation, HMTA was added as catalyst that resulted in a considerable reduction of the gelation time and condensation promoting.
It was considered that the hydrolysis and condensation rates of TEOS were greatly dependent upon the catalyst and the pH value (Brinker, Scherer, 1985). Thus, for pH values below 7, hydrolysis rate increased with decreasing pH, but condensation rate decreased and reached its lowest point at pH=2, the isoelectric point for silica. In both steps in the previous work the pH was bellow 7 and subsequently decreased with increasing OA content.
Given the fact that SiC, is a refractory material which shows a high thermal conductivity, and because of its properties of particle strength and attrition resistance, mesoporous SiC is expected to have extensive application in harsh environments such as catalyst, sorbent or membrane support (Methivier et al, 1998; Keller et al, 1999; Pesant et al, 2004).
Nevertheless, SiC applications as catalyst carrier was limited due to the fact that the specific surface area reachable for this material was rather low. It was shown that the sol-gel process is a promising route to prepare high surface area SiC materials. (G. Q. Jin, X. Y. Guo, 2003) have investigated a modified sol-gel method to obtain mesoporous silicon carbide. As a first step, a binary sol was prepared starting from TEOS, phenolic resin and oxalic acid. Nickel nitrate was used in the sol-gel process as a pore-adjusting reagent. Secondly, a carbonaceous silicon xerogel was formed by the sol condensation with a small amount addition of

hexamethylenetetramine in order to accelerate the condensation of the sol. Finally, mesoporous SiC was obtained with a surface area of 112 m^2/g and an average pore diameter of about 10 nm by carbothermal reduction of the xerogel at 1250°C in an argon flow for 20h. Even though, the mechanism of formation of mesoporous SiC is not yet well defined, interestingly, it was found that the surface areas and pore size distributions are nickel nitrate content dependent.

However, this process is very time consuming and necessitates special conditions, such as flowing argon (40cm^3/min). Additionally, the carbothermal reduction of the xerogel is carried out at 1250°C for a relatively long holding time.

(Y. Zheng et al, 2006) prepared a carbonaceous silicon xerogel starting from TEOS and saccharose as silicon and carbon sources respectively. Then the xerogel was treated by the carbothermal reaction at 1450°C for 12h to prepare a novel kind of β-SiC. The characterization of the purified sample revealed mesoporous material nature with a thorn-ball-like structure and a higher surface area of 141 m^2/g. Moreover, the as obtained mesoporous SiC material, revealed two different kinds of pores, with 2-12 nm sized mesopores in the thorn-like SiC crystalloids and 12–30 nm sized textural mesopores in the thorn-ball-like SiC.

Even though the mechanism formation of mesoporous β-SiC is not yet understood, SiC formation could be attributed to either the reaction of SiO with C or SiO with CO in the carbothermal reduction. Nevertheless, it was assumed that the thorn-ball-like β-SiC was probably produced by both reactions. Indeed, it is believed that as a first step, the reaction of gaseous silicon monoxide with carbon results in the formation of thorn-like β -SiC crystalloids whereas, the second reaction of gaseous silicon monoxide with carbon monoxide contributes to the thorn-like β -SiC crystalloids connections to form the thorn-ball-like β -SiC.

(R. Sharma et all, 2008) reported a new and simple sol-gel approach to produce a simultaneous growth of nanocrystalline SiC nanoparticles with the nanocrystalline silicon oxide using TEOS, citric acid and ethylene glycol. After the gel development, a black powder was obtained after drying at 300°C. The powder was subsequently heat treated at 1400°C in hydrogen atmosphere. Interestingly, it was found that under these working conditions, crystalline silicon oxide was formed instead of amorphous silicon oxide which is normally found to grow during the gel growth technique.

On the other hand, SiC is considered to be one of the important microwave absorbing materials due to its good dielectric loss to microwave (Zou et al. 2006). In microwave processing, SiC can absorb electromagnetic energy and be heated easily. It has a loss factor of 1.71 at 2.45 GHz at room temperature. And the loss factor at 695°C for the same frequency is increased to 27.99. This ability for microwave absorption is due to the semiconductivity of this ceramic material (Zhang et al, 2002).

Moreover, SiC can be used as microwave absorbing materials with lightweight, thin thickness and broad absorbing frequency. Since pure SiC posses low dielectric properties that gives barely the capacity to dissipate microwave by dielectric loss, therefore, doped SiC was used in order to enhance the aimed properties. The most applied technique for N-doped SiC powder consists in laser-induced gas-phase reaction (D. Zhao et al, 2001; D.-L. Zhao et al, 2010).

(D. Zhao et al, 2001) prepared nano-SiC/N solid solution powders by laser method. The dielectric properties were measured at a frequency range of 8.2-12.4 GHz.

The interaction between electromagnetic waves and condensed matter can be described by using complex permittivity, ε* (ε* = ε′ + iε″, where ε′ being the real part and ε″ the imaginary part).
Table 7 gives the dielectric constants and the dissipation factors tg δ of Si/C/N compared to bulk SiO_2, hot-pressed SiC, Si_3N_4 and nano SiC particles (D. Zhao et al, 2001).

	Dielectric constants (ε)	**Dissipation factors (tg δ)**	**Frequency (GHz)**
Nano-SiC/N solid solution powder	ε′ = 46.46-27.69 ε″ = 57.89-38.556	1.25-1.71	8.2-12.4
Nano-SiC/N solid solution powder embedded in paraffin wax matrix	ε′ = 5.79-6.33 ε″ = 3.51-4.31	0.61-0.68	8.2-12.4
Nano SiC particles embedded in paraffin wax matrix	ε′ = 1. 97-2.06 ε″ = 0.09-0.19	0.045-0.094	8.2-12.4
Bulk SiO_2	8.32	0.12	10
Hot-pressed SiC	9.47	0.003	10
Bulk Si_3N_4	3.8	0.002	10

Table 7. Dielectric properties of nano-SiC/N solid solution powders compared to bulk SiO2, hot-pressed SiC, Si_3N_4 and nano SiC particles (D. Zhao et al, 2001).

The dielectric properties of the nano-SiC/N solid solution powder are very different from those of bulk SiC, Si_3N_4, SiO_2 and nano SiC. The ε′, ε ″ and tg **δ** of nano-SiC/N solid solution powder are much higher than those of nano SiC powder and bulk SiC, Si_3N_4 and SiO_2, particularly the tg **δ**. The promising features of nano-SiC/N solid solution powder would be attributed to more complicated Si, C, and N atomic chemical environment than in a mixture of pure SiC and Si_3N_4 phase. In fact, in the as obtained solid solution powder, the Si, C, and N atoms were intimately mixed. Even though, the amount of dissolved nitrogen in SiC-N solid solution has not been studied efficiently, where (Komath, 1969) has reported that the nitrogen content of the solid solution is at most about 0:3 wt%, it is supposed that the amount of dissolved nitrogen is larger than that reported. Consequently the charged defects and quasi-free electrons moved in response to the electric field, and a diffusion or polarization current resulted from the field propagation. Since there exists graphite in the nano Si/C/N composite powder, some charge carries are related to the sp^3 dangling bonds (of silicon and carbon) and unsaturated sp^2 carbons. Whereas, the high ε″ and loss factor tg δ were due to the dielectric relaxation.
Owing to the above mentioned sol-gel process advantages, nanocomposite materials are good candidates for sol-gel processing. Moreover, the doping of SiC can be carried out by the homogeneous sol system derived from initial liquid components, and that the sol-gel processing is rather simple.
(B. Zhang et al, 2002), synthesized nano-sized SiC powders by carbothermal reduction of SiO_2 and SiO_2–Al_2O_3 xerogels. This latter was prepared by mixing TEOS, saccharose and some Al_2O_3 powders. The xerogels were subsequently heated at 1550°C for 1h in argon or nitrogen atmosphere to synthesize SiC. It was found that aluminum and nitrogen have

important effects on the polytypes of SiC powders. In the presence of aluminium, the polytype of l2H SiC powders were obtained, whereas, 21R SiC was synthesized under the nitrogen atmospheres (table 8). During the synthesis of silicon carbide, Al_2O_3 is reduced by carbon and forms carbide. At the same time, aluminium dopes into SiC and forms solid solution. Thus, aluminium atoms replace atoms of silicon in the solid solution and induce vacancies of carbon. The lattice parameters were decreased with the increasing of aluminium content. On the contrary, when SiC powders are synthesized in nitrogen atmosphere, nitrogen atoms replace some carbon atoms and form silicon vacancies. The synthesized β-SiC powder has much higher relative permittivity (ε'_r = 30~50) and loss tangent (tg δ = 0.7~0.9) than all of the α-SiC powders, though the α-SiC powders with 5.26 mol% aluminium possess higher conductivities. In fact it was establish that for Al-doped SiC powders, the relative permittivities and loss tangents are in an opposite measure of the aluminium content. For the powders with the same aluminium content, the samples synthesized in nitrogen atmosphere have smaller values for ε'_r and tg δ than those obtained in argon atmosphere in the frequency range of 8.2-12.4 GHz. The fundamental factor on these dielectric behaviours is ion jump and dipole relaxation, namely the reorientation of lattice defect pairs (V_{Si}–V_C , Si_C–C_{Si}). In fact, aluminium and nitrogen decrease the defect pairs that contribute to polarization. With the increase of the aluminium content and the doping of nitrogen, the conductivity of SiC rises, but the relative dielectric constant and loss tangent decrease.

Sample	Atom ratio of Al-Si	Reaction atmosphere	SiC polytype	DC resistivity (Ω cm)	Calculated loss tangent for 10 GHz
1	0	Argon	3C	557.9	$8.00x10^{-2}$
2	2.63:100	Argon	12H	1803.5	$8.78x10^{-2}$
3	5.26:100	Argon	12H	511.3	$3.57x10^{-1}$
4	2.63:100	Nitrogen	21R	1181.7	$1.84x10^{-1}$
5	5.26:100	Nitrogen	21R	77.5	$4.06x10^{-1}$

Table 8. DC resistivities and calculated loss tangent of SiC powders as a function of the alumina content (B. Zhang et al, 2002).

Besides the p-type doping by Al, boron atoms can substitute preferably the silicon atoms of SiC lattice. (Z. Li et al, 2009) investigated the effects of different temperatures on the doping of SiC with B. The authors synthesized B-doped SiC powders by sol-gel process starting from the mixture sol of TEOS and saccharose as silicon and carbon sources, respectively, and tributyl borate as dopant at 1500 °C, 1600 °C, 1700 °C and 1800 °C. It was proved that C-enriched β-SiC is completely generated when the temperature is 1700°C and SiC(B) solid solution is generated when the temperature is 1800 °C. The powders synthesized at 1700 °C had fine spherical particles with mean size of 70 nm and narrow particle size distribution. On the contrary, few needle-like particles were generated in the powders synthesized at 1800 °C which is believed to be caused by the doping of B. Thus it is considered that the formed SiC(B) solid solution suppresses the anisotropic growth of SiC whiskers.
The electric permittivities of SiC samples were determined in the frequency range of 8.2–12.4 GHz. Results showed that the SiC(B) sample has higher values in real part ε′ and imaginary part ε″ of permittivity. The average values of ε′ and ε″ for the sample synthesized

at 1700 °C were 2.23 and 0.10, respectively. It was also noticed that both ε′ and ε″ have increased for the sample synthesized at 1800 °C, and particularly the ε″ was nearly 2.5 times greater than that of the sample synthesized at 1700 °C. This can suggest an improved capacity of dielectric loss in microwave range.
The basic factor on these dielectric behaviours is that for a temperature heat of 1800°C which generates the SiC(B) solid solution, there exist bound holes in SiC with acceptor doping. Under the alternating electromagnetic field, these bound holes will migrate to and fro to form relaxation polarization and loss, thus leading to higher ε′ and ε″ of the sample at 1800 ◦C.

4.4 Liquid phase sintering SiC technique

Since SiC possesses a strongly covalent bonding (87%), which is the source of intrinsically high strength of SiC sintered bodies, thus, it is difficult to obtain a fully dense bulk material without any sintering additives.
The sintering of SiC is usually performed at very high temperatures which could reach 2200°C in the solid state with the addition of small amounts of B and C. However, SiC based ceramics boron- and carbon-doped have poor or, at the best, moderate mechanical properties (flexural strength of 300-450 MPa and fracture toughness of 2.5-4 MPa.$m^{1/2}$) (Izhevsky et al, 2000).
Over the last three decades considerable effort has been spent in order to decrease the sintering temperature and to enhance the mechanical properties of silicon carbide ceramics. This effort was based on using sub-micron size, highly sinterable SiC powders and sintering additives able to advance the density of the bulk material and more over to improve or at least to preserve the relevant mechanical properties.
The most effective sintering aids in lowering the sintering temperature and providing the micostructure resistant to crack propagation have been completed by adding the metal oxides Al_20_3 and Y_2O_3 (Omori, Takei, 1982).
Thus the addition of suitable sintering additives leads to dense, fine grained microstructures that result in improved sintered material strength. Nevertheless, these additives are subject to secondary phases' formation at the grain boundaries that frequently cause loss of high temperature strength (Biswas, 2009).
The innovative approach of SiC sintering in the presence of a liquid phase was introduced by (Omori, Takei, 1988) in the early 1980s by pressureless sintering of SiC with Al_20_3 combined with rare earth oxides. Since this initiation several works have been done and have demonstrated that whatever is the starting silicon carbide phase (α or β), SiC was successfully highly densified by pressureless sintering with the addition of Al_20_3 and Y_2O_3 at a relatively low temperature of 1850 ~ 2000°C.
Since its initiation, liquid-phase-sintered (LPS) silicon carbide with metal oxide additives such as Y_2O_3 and Al_20_3 has attracted much attention because it possesses a remarkable combination of desirable mechanical, thermal and chemical properties making it a promising structural ceramic.
One approach to enhance the mechanical properties of β-SiC is to control the gas atmosphere during the sintering. For instance it has been found that sintering LPS SiC in N_2 atmosphere suppresses the α→ β phase transformation and their grain growth, while Ar atmosphere enhances this phase transformation by the formation of elongated grains (Nader et al, 1999; Ortiz et al, 2004).

In this context, (Ortiz et al, 2004) studied the effect of sintering atmosphere (Ar or N_2) on the room- and high-temperature properties of liquid-phase-sintered SiC. It was shown that LPS SiC sintered in N_2 atmosphere possesses equiaxed microstructures and interestingly nitrogen was incorporated in the intergranular phase making the LPS SiC ceramic highly refractory. Moreover, this results in coarsening-resistant microstructures that have very high internal friction (Ortiz et al, 2002).
Two individual batches were prepared, each one containing a mixture of 73.86 wt.% β-SiC , 14.92 wt.% Al_2O_3 and 11.22wt.% Y_2O_3 in order to result in 20 vol.% yttrium aluminium garnet (YAG) in the LPS SiC bodies. Several pellets were prepared and then cold-isostatically pressed under a pressure of 350 Pa before being sintered at 1950°C for 1h in either flowing Ar or N_2 gas atmospheres. Table 9 summarizes the studied mechanical properties at room temperature of the LPS SiC ceramics in Ar atmosphere (Ar-LPS SiC) and in N_2 atmosphere (N_2-LPS SiC) where both materials have densities in excess of 98% of the theoretical limit of 3.484 g cm^{-3}.
At room temperature the microstructure of the LPS SiC sintered in N_2 atmosphere, was characterized by equiaxed grains, as compared with the LPS SiC in Ar-atmosphere which presented rather highly elongated SiC grains.

	Vickers hardness H (GPa)	**Vickers indentation toughness K_{IC} (MPa.$m^{1/2}$)**	**Hertzian indentation**
Ar-LPS SiC	17.6±0.3	3.3±0.1	**"quasi-ductile" material**
N2-LPS SiC	**20.7±0.6**	**2.2±0.1**	**Less "quasi-ductile" material**

Table 9. Mechanical properties of the SiC ceramics sintered in flowing Ar and N_2 gas atmospheres (Ortiz et al, 2004).

At high temperature (1400°C) the LPS SiC specimens presented equiaxed-grained structures with a highly viscous N_2-LPS SiC intergranular phase. This microstructure resulted in high resistance to high temperature deformation to a greater extent than Ar-LPS SiC, before the ultimate compressive strength is reached. Table 10 reports the mechanical properties of LPS SiC ceramics in Ar and N_2 gas atmospheres, measured at 1400°C.

	Elasticity limit deformation % ε_e	**Ultimate compression strength σ_{UCS} (MPa)**	**Total strain at catastrophic failure % ε_F**
Ar-LPS SiC	~ 1.8	630	**~ 11.4**
N_2-LPS SiC	**~ 1.8**	**870**	**~ 6**

Table 10. Mechanical properties of LPS SiC ceramics in Ar and N_2 gas atmospheres measured at 1400°C (Ortiz et al, 2004).

The relevant contrast in the mechanical properties of the LPS SiC in different atmospheres (N_2 and Ar) was argued to be due to the elongated-grained microstructure and the less viscous intergranular phase devoid of nitrogen.

In another approach (Padture, 1994) succeeded in enhancing the fracture toughness, by seeding the β-SiC powder with 3~5 wt. % of α-SiC through the LPS SiC technique. Additionally, the temperatures were maintained higher than 1900°C for different durations in order to allow the growth of elongated α-SiC grains. Nevertheless, this process despite the fact provides SiC ceramics with improved fracture toughness, it involves high temperatures (> 1900°C) and consequently beats the principle of the LPS process for being low temperature as well as low energy consumption.

(Wang, Krstic, 2003) studied the effect of Y_2O_3 addition and the total oxide volume fraction (Y_2O_3 + Al_2O_3) on mechanical properties of pressureless sintered β-SiC ceramics at low temperature. It was demonstrated that the increase in strength with yttria (Y_2O_3) content is directly related to the increase in relative density of the sintered specimens, which, in turn is related to the level of Y_2O_3 addition. The study of the fracture toughness of SiC ceramics with oxide addition revealed that with increasing the oxide content, the fracture toughness increases and reached a maximum of about 4.3 MPa. $m^{1/2}$ achieved at ~ 14 vol.% of oxide added for samples sintered at 1850°C. This is mostly related to crack deflection mechanism's toughening which occurs when the crack changes its direction as it encounters the SiC grains and the grain boundary phase. Moreover, the mechanism of toughening is further enhanced by thermal mismatch between SiC and the intergranular YAG phase at the grain boundaries this leads to the crack's progress along the grain boundaries (Kim D. Kim C., 1990).

An alternative promising strategy to improve the mechanical properties of β-SiC is to adjust the volume fraction and composition of the boundary phase so as to generate the microstructure with high density and resistance to crack propagation. The variation of the α-SiC and β-SiC proportions of the starting powders mixture is considered to be an efficient way of adjusting both the microstructure and the mechanical properties of the SiC ceramic. (Wang, Krstic, 2003).

According to this approach, (Lee et al, 2002) investigated the effect of the starting phase of the raw material on the microstructure and fracture toughness of SiC ceramic by varying the mixed ratio of α-SiC and β-SiC powders. The authors prepared several samples by altering the β/α phase ratio of SiC starting powder from 0 to 100 vol. % and adding 2 mol % of yttrium aluminium garnet and 2.5 wt. % polyethyleneglycol (PEG). The mixtures were then compacted and hot pressed at 1850°C for 30 min at a pressure of 50 MPa and subsequently sintered at 1950°C for 5h. The densities of the resulting compacted powders were higher than 95 % of theoretical density regardless of the starting phase. Most sintered SiC specimens enclosed elongated grains with rod-like type. However it was noticed that the amount of elongated grain and its aspect ratio was changed with the ratio of α- anf β-SiC in the starting powder. Elongated grains were formed by the β→α phase transformation with a 4H polytype and anisotropic grain growth during heat treatment. It was concluded from this study, that specimen containing 50 vol.% β-SiC in the starting powder showed the highest values of volume fraction, maximum length and aspect ratio for elongated grains. This specimen revealed also the highest fracture toughness of 6.0 MPa. $m^{1/2}$ which is due to the elongated grains induced crack deflection during crack propagation.

In table 11 are reported some mechanical properties of LPS SiS as a function of different sintering aids.

References	Technique	Sintering additives	Hardness H (GPa)	Fracture Toughness (MPa. $m^{1/2}$)	Density
(Chen, Zeng, 1995)	Pressureless sintering SiC	Al_2O_3 + HoO3 (eutectic composition)	17.47	3.68	Up to 3.764 g/cm^3
(Chen, 1993)	Pressureless sintering SiC	Al_2O_3 + SmO3 (eutectic composition)	17.1	4.6	92.6 %
(Hidaka et al,2004)	Hot pressing at 1950°C and P=39 MPa	(Al_2O_3 + Y^{3+} ions) /Polytitanocarbosilane by infiltration	19 - 21	5.9	95 – 98 %
(Scitti et al, 2001)	Hot pressing at 1850-1950°C Annealing (1900°C/3 or 2h)	Al_2O_3 + Y_2O_3	22 24.5-25	2.95 – 3.17 Up to 5.5	Up to 99.4 % (3.24 g/cm^3) 3.22 g/cm^3
(Wang, Krstic, 2003)	Pressureless sintering β-SiC at 1850°C	Y_2O_3 in (Al_2O_3 + Y_2O_3)	22	4.3	~ 98 %
(Mulla, Krstic, 1994)	Pressureless sintering β-SiC at 2050°C	Al_2O_3	_	6	97-98 %
(Hirata et al, 2010)	Hot pressing at 1900-1950°C and P=39 MPa	Al_2O_3 + Y_2O_3	_	6.2	97.3-99.2

Table 11. Mechanical properties of LPS-SiC as a function of different sintering aids.

It could be concluded that, densities in excess of 99% of the theoretical limit can be easily achieved by carefully choosing the composition of the liquid phase and the packing powder configuration (Jensen et al, 2000).

On one hand, the sintering mechanism in the pressureless liquid-phase sintering to full dense SiC with Al_2O_3 and Y_2O_3 additions is considered to be attributed to liquid-phase-sintering via the formation of an eutectic liquid between Al_2O_3 and Y_2O_3 to yield yttrium aluminium garnet, or YAG, based liquid phase. On the other hand, the hardness was mainly related to reduction of secondary phases which generally decrease such property.

Finally, the increase in toughness is related not only to grain morphology but also to second phase chemistry, thus a suitable choice of thermal treatment parameters that modify second phase chemistry without excessive grain growth can theoretically lead to a reinforced microstructure with slight or no strength decrease.

4.5 Mechanical alloying process for SiC synthesis

Nanostructured silicon carbide attracted considerable attentions from the materials and device communities and have been studied intensively in the past decade due to its unique properties and wide applications in microelectronics and optoelectronics (Li et al, 2007).

In fact, it was reported that inorganic structures confined in several dimensions within the nanometer range, exhibit peculiar and unique properties superior to their bulk counterparts. These unique properties can be attributed to the limited motion of electrons in the confined dimensions of the nanomaterial (Barth et al, 2010). However the transition from fundamental science to industrial application requires an even deeper understanding and control of morphology and composition at the nanoscale. Size reduction of well known materials into the nanometre regime or the realization of novel nanostructures can improve device performance and lead to novel discoveries (Barth et al, 2010).

Among the techniques that produce nanostructured materials the mechanical alloying is considered as a powerful process for producing nanomaterials at room temperature with low cost and at a large scale (Basset et al, 1993). However, this process also exhibits disadvantages such as the contamination of both the milling media and the mill atmosphere. During mechanical alloying, two essential processes are involved: cold welding and fracturing of powder particles. Thus after a certain activation time during this process, while the particles size decreases during milling, the number of chemically active defect sites increases. Moreover, towards the milling process which results in repeated fracturing and rewelding of particles the activated zones are continuously increased leading to a considerable temperature decrease for reactions occurring in a planetary mill. For more details see (D. Chaira et al, 2007; Benjamin, 1970). Thus, the normally proceeded reactions at high temperature become possible at low temperature with this technique which constitutes the major advantage of the MA. Then, the restriction caused by thermodynamic phase diagram is overcome by mechanical alloying.

Mechanical alloying as a complex process, it involves therefore, the optimization of a number of variables to achieve the desired product phase and/or microstructure.

The most important parameters that have an effect on the final constitution of the powder are:

. type of mill,
. milling container,
. milling speed,
. milling time,
. type, size, and size distribution of the grinding medium,
. ball-to-powder weight ratio,
. extent of filling the vial,
. milling atmosphere,
. process control agent,
. number and diameter of balls,
. temperature of milling.

Actually these parameters are not completely independent. For more details see (Suryanarayana, 2001).

The applications of MA are numerous, for instance it was used for the synthesis of nanostructured carbides (El Eskandarany et al, 1995; Ye, Quan, 1995; Razavi et al, 2007), nitrides (Calka et al, 1992), composites (Shen et al, 1997) and solid solutions (Li et al, 2002).

Since the work initiated by (Benjamin, 1970; Benjamin, Volin, 1974), MA has attracted more and more attentions due to the all above cited advantages. (Le Caer et al, 1990) synthesized a series of metal carbides and silicides by ball milling mixtures of elemental powders at room temperature with a vibratory mill at fixed miling durations. Whereas, (D. Chaira et al, 2007) used a specially built dual-drive planetary mill to synthesize nanostructured SiC starting from elemental silicon and graphite mixed in 1:1 atomic ratio. The used mill design follows closely the patent design of (Rajamani et al, 2000). The weighed ball-to-powder ratio was 20 to 1 and the mechanical alloying was performed in a planetary ball mill with a critical speed of 63% by using two different balls' diameter (6 and 12 mm). It was shown that in both cases and for the end product milled for 40h, peaks corresponding to Si_5C_3, SiC and β-SiC were detected. Nevertheless, the rate of SiC formation during milling as well as the impact's intensity to dislodge any coating that forms on the ball's surface was found to be better with 12 mm diameter ball. The mechanism of SiC formation under the experimental conditions indicated above corresponds to the following: during the early stage of milling (10h), the powder particles were mechanically activated by Si and C particles mixing forming thus composite particles. Later on, after about 20h of milling, the solid-state reaction started and significant amounts of SiC are produced. Based on the X-ray line broadening it was concluded that the product compound has reduced crystallite size as well as accumulation of lattice strain. The crystallite size was found to be decreased to 10 nm after 40h of milling. Whereas, (El Eskandarany et al, 1995), while using a commercially available vibrating ball mill obtained pure stoichiometric β-SiC powders after 300h of mechanical alloying duration. They started from a mixture of equiatomic Si and C with a ball-to-powder weight ratio of 6 to 1. Under the selected mechanical alloying conditions and at the early stage of MA (after about 6h), the TEM observation revealed that the powders are still a mixture of polycrystalline Si and C. After about 12h of MA the Si and C powders particles were blended together to form composite particles of Si/C. For the alloy MA for 48h a solid-state reaction took place resulting in the β-SiC phase formation. Finally the complete β-SiC phase powder was obtained after 300h of MA which exhibited a homogeneous, smooth spherical shape with an average particle diameter of less than 0.5 μm. A fine cell-like structure with nanoscale dimensions of about 7 nm was also obtained. Table 12 summarizes the mechanism of β-SiC formation with the selected MA parameters in (El Eskandarany et al, 1995).

MA Durations (ks)	**Powder constitution**	**Morphology**	**Particle size**
0	Si and C elemental powders	bulky	300-350 mesh
86	Si/C composite particles	Rod or ellipsoid	6 μm
360	β-SiC and unreacted Si and C	Uniform equiaxed particles	< 1 μm
1080	Pure β-SiC	Spherical with smooth surface	< 0.5 μm

Table 12. The mechanism of β -SiC formation during MA (El Eskandarany et al, 1995).

It is worth to note that, as in this study when a sapphire vial and balls were used there were non contaminants detected coming from the milling media except 0.8 at. % content of oxygen detected in the as milled product, coming probably from the atmosphere medium. In order to study the stability of the MA β-SiC at elevated temperatures, the as obtained end product was annealed at 1773 K and it was demonstrated that there was no transformation to any other phases up to this temperature.

(Lu, Li, 2005) investigated the effect of different Si powders for the synthesis of $Si_{50}C_{50}$ by MA using a conventional planetary ball mill. In order to do so, both Si wafers previously milled for 5h into small particles (particle size of about 1 μm) and commercially available Si powder were separately ball milled with graphite powder under the same experimental conditions. It was shown that the end products obtained from different Si powders were almost similar. Under the selected milling conditions and with a powder-to-ball mass ratio of about 1:20, the SiC phase starts to form after about 100h of milling duration. The reaction between C and Si was gradual and completed after 180h of MA where pure and fine SiC powders were obtained.

(Aberrazak, Abdellaoui, 2008) obtained equiatomic nanostructured SiC starting from elemental Si and C powders, using a commercialized planetary ball mill with milling conditions corresponding to 5.19 W/g shock power (M. Abdellaoui, E. Gaffet, 1994; M. Abdellaoui, E. Gaffet, 1995). Under the optimized milling conditions a pure SiC phase was formed after just 15h. The reaction between C and Si was proved to be gradual and started after about 5h of MA with a SiC weight content around 1 %. This proportion increased to about 66 % after 10h alloying and to about 98 % after 15 h alloying. Contrary to the previous cited works a steady state was reached by (Aberrazak, Abdellaoui, 2008) after only 20 h of alloying duration and was characterized by a crystallite size of about 4nm. The SEM characterization revealed that the powder exhibited homogeneous distribution of the particles with 0.3 μm in size.

(Ghosh, Pradhan, 2009) reproduced the same milling duration for the synthesis of a pure β-SiC phase by high-energy ball-milling. It was revealed from this study that a development of thin graphite layer and amorphous Si were detected after 3 h of milling. Whereas, the formation of a nanocrystalline SiC phase started, by re-welding mechanism of amorphous Si and graphite layers, within 5 h of milling. Thanks to the microstructural characterization of the mechanically alloyed sample by Rietveld's analysis, it was shown that at the early stage of milling, graphite layers are distributed on the Si nano-grain boundaries as very thin layers. Finally, the complete formation of nanocrystalline SiC phase was accomplished after 15 h of milling. For the Rietveld analysis investigation, conversely to the fitting done without considering the amorphous phase contribution, the fitting profile presented better quality when amorphous silicon was taken in account.

Same calculated lattice parameters of β-SiC are reported in table 13.

β-SiC Lattice constant	**(El-Eskandarany et al, 1995) calculated**	**(Aberrazak, Abdellaoui, 2008) calculated**	**(Li, Bradt, 1986) Reported literature**	**(Liu et all, 2009) Reported literature**
a = b= c (nm)	0.4357	0.4349	0.4358	0.4348

Table 13. β-SiC lattice parameter as calculated for materials obtained by MA and as reported in the literature.

The lattice parameters variations revealed in table 2 is mainly related to the severe deformation on powder particles which occurs during the mechanical alloying. Moreover, with increasing the milling time, the crystalline defects, such as point defects and dislocations, increase too.

Mechanically alloyed SiC can also be used as reinforcement in the Al matrix. In fact, Al/SiC has received particular interests during recent years due to their high specific modulus, high strength and high thermal stability. One of the largest applications of this composite is the automobiles industry such as electronic heat sinks, automotive drive shafts, ground vehicle brake rotors, jet fighter aircraft fins or explosion engine components (Clyne, Withers, 1993).

Due to Al/SiC remarkable properties, considerable effort has been developed for its fabrication. The most used technique for composites fabrication is casting. However, even though this technique is the cheapest one, it is difficult to apply for the synthesis of Al/SiC composites owing to the extreme gap difference in the thermal expansion coefficients between Al and SiC. In addition there is a poor wettability between molten Al (or Al alloys) and SiC. Moreover, undesirable reaction between SiC and molten Al, might occurs resulting in brittle phases' formation of Al_4C_3 and Si. In order to circumvent to these main drawbacks, solid state process such as mechanical alloying (MA) is considered as a promising way to avoid brittle phases and particle agglomerations during fabrication of Al/SiC composite (Saberi et al, 2009).

(Chaira et al, 2007) prepared Al/SiC composite by mixing nanostructured SiC powder, obtained by MA, with Al particles. The mixture was then sintered at 600°C for 1h to obtain Al-10 vol.% SiC composite. The studied SEM micrographs revealed a good compatibility particles as well as a good interfacial bond between Al matrix and SiC respectively. Moreover, no cracks or voids were present. It is worth to know that the interface between the metal and the particle is decisive for the determination of the overall properties of metal matrix composite. In fact, it was reported that a well-bonded interface facilitates the efficient transfer and distribution of load from matrix to the reinforcing phase, which results in composite strengths enhancement. For the two studied specimens differing in SiC proportion in the prepared composite (10 and 20 vol. %), a maximum of 90 % of theoretical density was achieved.

The co-effect of varying process parameters of milling on the evolution of powder's properties was not well established up to now. (Kollo et al, 2010) investigated the effect of milling parameters on the hardness of Al/SiC composite obtained by milling aluminium powders with 1 vol. % of nanostructured silicon carbide using a planetary ball mill. The varied milling parameters were such like rotation's disc speed, milling time, ball diameter, ball-to-powder ratio and processing control agent (stearic acid or heptane).

The studied parameters revealed that the hardness of the compacted materials when milled with heptane, as processing control agent, was not greatly influenced by the input energy. Besides, there was no sticking of aluminium on the vessel and the balls. Whereas, when using stearic acid, a remarkable difference of hardness response was found. Indeed, it is well established that stearic acid has a tendency to react during high-energy milling, in introducing carbon to the powder mixture. Consequently, it is supposed that reaction kinetics in addition to mixing is contributing to the hardening of the densified materials where a density range of 92-95 % of the theoretical was achieved. On the other hand, it was shown that the milling speed has a higher influence when the milling is performed with smaller balls, yielding thus to higher hardness values. It was also found that the hardness generally increases with the time and the speed of milling, while, milling speed has a higher

influence when the milling is performed with smaller balls. Whereas, for vial filling volume, depending on the ball size, a local minimum in filling parameter was found.

Table 14 reports Vickers hardness of different Al/SiC composites prepared by MA.

Al/SiC composition	Technique	Vickers hardness (Hv)	Reference
Al-20 vol.% SiC	(Al + nanoSiC) Sintered at 600°C for 1h	40	Chaira et al, 2007
Al/SiC composite	SiC incorporated by mechanically stirring the fully molten Al	36±2 - 39±1	Tham et al, 2001
Al–1 vol.% nano SiC	(Al + nanaoSiC) hot pressed	163	Kolloa et all, 2010

Table 14. Microhardness of different Al/SiC composites obtained by MA.

(Chaira et al, 2007), demonstrated that with increasing sintering temperature, the hardness of Al-SiC composites increased too due to good compatibility of Al and SiC particles. However, the hardness values of the obtained composite remained by far lower than the one given by (Kolloa et all, 2010) who had studied and optimized the milling's parameters on the hardness of the material. Moreover, a better density was also achieved, a property which is also related to the hardness of the material.

5. Conclusion

Silicon carbide can occur in more than 250 crystalline forms called polytypes. The most common ones are: 3C, 4H, 6H and 15R. Silicon carbide has attracted much attention a few decades ago because it has a good match of chemical, mechanical and thermal properties that makes it a semiconductor of choice for harsh environment applications. These applications include high radiation exposure, operation in high temperature and corrosive media. To obtain high-performance SiC ceramics, fine powder with narrow particles-size distribution as well as high purity are required. For this purpose, many effective methods have been developed.

The simplest manufacturing process of SiC is to combine silica sand and carbon in an Acheson graphite electric resistance furnace at temperatures higher than 2500 °C. The poor quality of the obtained product has limited its use for abrasive.

Sol-gel process has proved to be a unique method for synthesis of nanopowder, having several outstanding features such as high purity, high chemical activity besides improvement of powder sinterability. Nevertheless, this process suffers time consuming and high cost of the raw materials. On the other hand, mechanical alloying is a solid state process capable to obtain nanocrystalline silicon carbide with very fine particles homogeneously distributed at room temperature and with a low coast. Moreover this process has a potential for industrial applications.

Liquid-phase-sintered ceramics represent a new class of microstructurally toughened structural materials. Liquid phase sintering technique, for instance, is an effective way to lower the sinterability temperature of SiC by adding adequate additives in the appropriate

amounts. In fact, as the main factors affecting the improvements of the mechanical properties of the LPS-SiC, depend on the type and amount of sintering aids these latter have to be efficiently chosen. Whereas, physical vapor transport technique is versatile for film depositions and crystals growth. One of the large applications of PVT technique is crystalline materials production like semi-conductors. Indeed this method was considered to be the most popular and successful for growing large sized SiC single crystals.

6. References

a. Abdellaoui M., Gaffet E., (July, 1994), A mathematical and experimental dynamical phase diagram for ball-milled $Ni_{10}Zr_7$, *Journal of Alloys and Compounds*, 209, 1-2, pp: 351-361.

b. Abdellaoui M., Gaffet E., (March 1995), The physics of mechanical alloying in a planetary ball mill: Mathematical treatment , *Acta Metallurgica et Materialia*, 43, (3), pp: 1087-1098.

Abderrazak H., Abdellaoui M., (2008), Synthesis and characterisation of nanostructured silicon carbide, *Materials Letters*, 62, pp: 3839-3841.

Augustin G., Balakrishna V., Brandt C.D., Growth and characterization of high-purity SiC single crystals, *Journal of Crystal Growth,* 211, (2000), pp: 339-342.

Barrett D.L., McHugh J.P., Hobgood H.M., Hobkins R.H., McMullin P.G., Clarke R.C., (1993), Growth of large SiC single crystals*, Journal Crystal Growth*, 128, pp: 358-362.

Barth S., Ramirez F. H., Holmes J. D., Rodriguez A. R., (2010), Synthesis and applications of one-dimensional semiconductors, *Progress in Materials Science*, 55,pp: 563-627.

Basset D., Mattieazzi P., Miani F., (August, 1993), Designing a high energy ball-mill for synthesis of nanophase materials in large quantities, *Materials Science and Engineering: A*, 168, 2, pp: 149-152.

Benjamin J. S., (1970), Dispersion strengthened superalloys by mechanical alloying, *Metallurgical transactions*, 1, 10, pp: 2943-2951.

Benjamin J. S., Volin T. E., (1974), The mechanism of mechanical alloying, Metallurgical and Materials Transactions B, 5, 8, pp: 1929-1934

Biswas K., (2009), Liquid phase sintering of SiC-Ceramic, *Materials science Forum*, 624, pp: 91-108.

Brinker C.J., Clark D.E., Ulrich D.R. (1984) (Eds.), Better Ceramics Through Chemistry, North-Holland, New York.

Brinker C.J., Keefer K.D., Schaefer D.W., Ashley C.S., (1982), Sol-Gel Transition in Simple Silicates, *Journal of Non-Crystalline Solid*s, 48, pp.47-64

Brinker C. J., Scherer G. W., (1985), Sol→gel→glass: I. Gelation and gel structure. *Journal of Non-Crystalline Solids*, 70, pp: 301-322.

Bouchard D., Sun L., Gitzhofer F., Brisard G. M., (2006), Synthesis and characterization of $La_{0,8}Sr_{0,2}MO_{3-\delta}$ (M = Mn, Fe or Co) cathode materials by induction plasma technology, *Journal of thermal spray and technology*, 15(1), pp: 37-45.

Calka A, Williams J. S., Millet P., (1992), Synthesis of silicon nitride by mechanical alloying, *Sripta Metallurgica and Materiala,* 27, pp: 1853-1857

Casady J.B., Johonson R.W., (1996), Status of silicon carbide (SiC) as a wide-bangap semiconductor for high-temperature applications, A Review, *Solid State Electronics*, 39, pp: 1409-1422.

Čerović Lj., Milonjić S. K., Zec S. P, (1995), A comparison of sol-gel derived silicon carbide powders from saccharose and activated carbon, *Ceramics International*, 21, 27 l-276.

Chaira D., Mishra B.K., Sangal S., (2007), Synthesis and characterization of silicon carbide by reaction milling in a dual-drive planetary mill, *Materials Science and Engineering A,* 460–461, pp: 111–120.

Chen Z., (1993), Pressureless sintering of silicon carbide with additives of samarium oxide and alumina, *Materials Letters*, 17, pp: 27-30.

Chen Z., Zeng L., (1995), Pressurelessly sintering silicon carbide with additives of holmium oxide and alumina, *Materials Research Bulletin*, 30(3), pp. 256-70.

Clyne T. W., Withers P. J., An introduction to metal matrix composites, Cambridge University Press, Cambridge, ISBN 0521418089.

El Eskandarany M. S., Sumiyama K., Suzuki K., (1995), Mechanical solid state reaction for synthesis of β-SiC powders, *Journal of Materials Research*, 10, 3, pp: 659-667.

Ellison A., Magnusson B., Sundqvist B., Pozina G., Bergman J.P., Janzén E., Vehanen A., (2004), SiC crystal growth by HTCVD*, Materials Science Forum*, 457-460, pp: 9- 14.

Fend Z. C., (2004), SiC power materials: devices and applications. Ed. Springer series in material science, Springer-Verlag Berlin Heidelberg, ISBN: 3-540-20666-3.

Fu Q-G., Li H. J., Shi X. H., Li K. Z., Wei **J**., Hu Z. B., (2006), Synthesis of silicon carbide by CVD without using a metallic catalyst, *Matetrials Chemistry and Physics,* 100, pp: 108-111.

Ghosh B., Pradhan S.K., (July, 2009), Microstructural characterization of nanocrystalline SiC synthesized by high-energy ball-milling, *Journal of Alloys and Compounds,* 486, pp: 480–485.

Han R., Xu X., Hu X., Yu N., Wang J. Tan Y. Huang W., (2003), Development of bulk SiC single crystal grown by physical vapor transport method, *Optical materials*, 23, pp: 415-420.

Hidaka N., Hirata Y., Sameshima S., Sueyoshi H., (2004), Hot pressing and mechanical properties of SiC ceramics with polytitanocarbosilane, *Journal of Ceramic Processing Research*, 5, 4, pp: 331-336.

Hirata Y., Suzue N., Matsunaga N., Sameshima S., (2010), Particle size effect of starting SiC on processing, microstructures and mechanical properties of liquid phase-sintered SiC, *Journal of European Ceramic Society*, 30 pp: 1945-1954.

Humphreys R.G., Bimberg D. , Choyke W .J., Wavelength modulated absorption in SiC, *Solid State Communications*, 39, (1981), pp:163-167.

Izhevsky V. A., Genova L. A., Bressiani A. H. A., Bressiani J. C., (2000), Liquid-phase-sintered SiC. Processing and transformation controlled microstructure tailoring, *Materials Research*, 3(4) pp: 131-138.

Jensen R. P., Luecke W. E., Padture N. P., Wiederhorn S. M., (2000), High temperature properties of liquid-phase-sintered α-SiC, *Materials Science and Engineering*, A282, pp. 109-114.

Jin G. Q., Guo X. Y., (2003), Synthesis and characterization of mesoporous silicon carbide, *Microporous and Mesoporous Materials*, 60 (203), pp: 207-212.

Julbe A., Larbot A., Guizard C., Cot L., Charpin J., Bergez P., (1990), Effect of boric acid addition in colloidal sol-gel derived SiC precursors, *Materials and Research Bulletin*, 25, pp. 601-609.

Kamath G.S., (1968), International Conference on Silicon Carbide, Pennsylvania, USA, (1969), Special Issue to *Material Research Bulletin*, 4, S1-371, pp. S57–S66.

Kavecký Š., Aneková B., Madejová J., Šajgalík P., (2000), Silicon carbide powder synthesis by chemical vapor deposition from siliane/acetylene reaction system, *Journal of the European Ceramic Society,* 20, pp: 1939-1946.

Keller N. , Huu C. P., Crouzet C., Ledoux M. J., Poncet S. S., Nougayrede J-B., Bousquet J., (1999), Direct oxidation of H_2S into S. New catalysts and processes based on SiC support, *Catalyst Today*, 53, 535-542.

Klein L.C., Garvey G.J., (1980), Kinetics of the Sol-Gel Transition, *Journal of Non-Crystalline Solids*, (38-39), pp:45-50.

Kleiner S., Bertocco F., Khalid F.A., Beffort O., (2005), *Materials Chemistry and Physics*, 89, 2-3, pp: 362-366.

Kim D. H., Kim C. H., (1990), Toughening behavior of silicon carbide with addition of yttria and alumina, Journal of American Ceramic Society, 73, 5, pp. 1431-1434..

Kollo L., Leparoux M., Bradbury C. R., Jäggi C., Morelli E. C., (2010), Arbaizar M. R., Investigation of planetary milling for nano-silicon carbide reinforced aluminium metal matrix composites, *Journal of Alloys and Compounds*, 489, pp: 394-400.

Laube M., Schmid F., Pensl G., Wagner G., (2002), Codoping of 4H-SiC with N- and P-Donors by Ion Implantation, *Materials Science Forum*, 389-393, pp: 791-794..

Le Caer G., Bauer-Grosse E., Pianelli A., Bouzy E., Matteazzi P., (1990), Mechanically driven synthesis of carbides and sillicides, *Journal of Materials Science*, 25, 11, pp: 4726-4731.

Lee J-K., Park J-G., Lee E-G., Seo D-S., Hwang Y., (2002), Effect of starting phase on microstructure and fracture toughness of hot-pressed silicon carbide, *Materials Letters*, 57 pp: 203-208.

Lely J.A., Keram B.D., (1955), Darstellung von Einkristallen von Silizium Karbide und Beherrschung von Art und Menge der eingebauten Verunreinigungen, *Ber. Deut. Keram. Ges* 32, pp: 229-231.

Li J. L., Li F., Hu K., (December, 2002), Formation of SiC-AlN solid solution via high energy ball milling and subsequent heat treatment, *Materarials Science and Technology*, 18, pp: 1589-1592.

Li J., Tian J., Dong L., Synthesis of SiC precursors by a two-step sol-gel process and their conversion to SiC powders, (2000), Journal of the European Ceramic Society 77 pp: 1853-1857.

Li K. Z., Wei J., Li H. J., Li Z. J., Hou D. S., Zhang Y. L., (2007), Photoluminescence of hexagonal-shaped SiC nanowires prepared by sol-gel process, *Materials Science and Engineering*, A 460-461, pp: 233-237.

Li Z., Zhou W., Lei T., Luo F., Huang Y., Cao Q., (2009), Microwave dielectric properties of SiC(β) solid solution powder prepared by sol-gel, *Journal of Alloys and Compounds,* 475, pp: 506–509.

Li X. B., Shi E. W., Chen Z. Z., Xiao B., Polytype formation in silicon carbide single crystals, *Diamond & Related Materials*, 16, (2007), pp: 654-657.

Liu H. S., Fang X. Y., Song W. L., Hou Z. L., Lu R., Yuan J., Cao M. S., (2009), Modification Modification of Band Gap of β-SiC by N-Doping, *Chinese Physics Letters,* 26, 6, 067101-1-067101-4

Lu C. J., Li Z. Q., (2005), Structural evolution of the Ti-Si-C system during mechanical alloying, *Journal of Aloys and Compounds*, 395, pp: 88-92

Methivier Ch., Beguin B., Brun M., Massardier J., Bertolini J., (1998), Pd/SiC catalysts: characterisation and catalytic activity for the methane total oxidation , *Journal of Catalyst*, 173, pp: 374, 382.

Moore J. J., Feng H. J., (1995), Combustion synthesis of advanced materials: Part I. Reaction parameters, *Progress in Materials Science*, 39, (4-5), pp: 243-273.

Mulla M. A., Krstic V. D., (1994), Mechanical properties of β-SiC pressureless sintered with Al_2O_3 additions, *Acta metallurgica et materiala,* 42, 1, pp. 303-308.

Muranaka T., Kikuchi Y., Yoshizawa T., (2008), Akimitsu J., Superconductivity in carrier-doped silicon carbide, Science and Technolology of Advanced Materials*, 9, 044204, pp: 1-8.*

Nader M., Aldinger F., Hoffman M. J., (1999), Influence of the α/β-SiC phase transformation on microstructural development and mechanical properties of liquid phase sintered silicon carbide, *Journal of Materials Science*, 34, pp: 1197-1204.

Noh S., Fu X., Chen L., Mehregany M., (2007), A study of electrical properties and microstructure of nitrogen-doped poly-SiC films deposited by LPCVD, *Sensors and Actuators*, A 136, pp: 613–617.

O'Connor J.R., Smiltens J., Eds, Silicone Carbide, a High Temperature Semiconductor, Pergamon, Oxford, 1960.

Omori M., Takei H., (1988), Preparation of pressureless-sintered SiC--- Y_2O_3--- Al_20_3, Journal of Materials Science, 23, pp: 3744-3749.

Omori M., Takei H., (1982), Pressureless sintering of SiC, *Journal of American Ceramic Society*, 65(6), pp: C92.

a. Ohtani N., Katsuno M., Nakabayachi M., Fujimoto T., Tsuge H., Yaschiro H., Aigo T., Hirano H., Hoshino T., Tatsumi K., (2009), Investigation of heavily nitrogen-doped n^+ 4H-SiC crystals grown by physical vapor transport, *Journal of Crystal Growth*, 311, 6, pp: 1475-1481.

b. Ohtani N., Fujimoto T., Katsuno M., Yshiro H., in: Feng Z.C. (Ed), SiC Power Materials-Devices and Applications, Springer Series in Materials, 73, Springer, Berlin, 2004, p. 89.

Ortiz A. L., Bhatia T., Padture N. P., Pezzotti G., (2002), Microstructural evolution in liquid-phase-sintered SiC: III, effect of nitrogen-gas sintering atmosphere, *Journal of American Ceramic Society*, 88, pp: 1835-1840.

Ortiz A. L., M-Bernabé A., Lopez O. B., Rodriguez A. D., Guiberteau F., Padture N. P., (2004), Effect of sintering atmosphere on the mechanical properties of liquid-phase-sintered SiC, *Journal of European Ceramic Society*, 24, pp: 3245-3249.

Padture N. P., (1994), In-situ toughened silicon carbide, *Journal of American Ceramic Society*, 77(2), pp: 519-523.

Pensl G., Choyke W.J., Electrical and optical characterization of SiC, *Physics B*,185, (1993), 264-283.

Pesant L., Matta J., Garin F., Ledoux M.J., Bernhard P., Pham C., Huu C. P., (2004), A high-performance Pt/ß-SiC catalyst for catalytic combustion of model carbon particles (CPs), *Applied Catalysis A,* 266**,** pp: 21-27.

Polychroniadis E. K., Andreadou A., Mantzari A., (2004), Some recent progress in 3C-SiC growth. A TEM characterization, *Journal of Optoelectronics and Advanced Materials,* 6,1, pp: 47-52.

Rodeghiero E.D., Moore B.C., Wolkenberg B.S., Wuthenow M., Tse O.K., Giannelis E.P., (1998) Sol-gel synthesis of ceramic matrix composites, *Materials Science and Engineering A24*, pp: 11–21.

Raman V., Bahl O. P., Dhawan U., (1995), Synthesis of silicon carbide through the sol-gel process from different precursors, *Journal of Materials Science*, 30, pp: 2686-2693.

Rajamani, R.K., Milin L., Howell G., (2000), United States Patent no. 6,086,242.

Razavi M, Rahimipour M. R., Rajabi-Zamani A. H., (2007), Synthesis of nanocrystalline TiC powder from impure Ti chips via mechanical alloying, *Journal of Alloys and Compounds*, 436, pp: 142-145.

Rost H.-J, Doerschel J., Irmscher K., Robberg M., Schulz D., Siche D., (2005), Polytype stability in nitrogen-doped PVT—grown 2″—4H–SiC crystals, *Journal of Crystal Growth*, 275, pp: e451e-454.

Saberi Y., Zebarjad S.M., Akbari G.H., (may, 2009), On the role of nano-size SiC on lattice strain and grain size of Al/SiC nanocomposite, *Journal of Alloys and Compounds*, 484, pp: 637–640.

Scitti D., Guicciardi S., Bellosi A., (2001), Effect of annealing treatments on microstructure and mechanical properties of liquid-phase-sintrerd silicon carbide, *Journal of European Ceramic Society*, 21, pp: 621-632.

Shaffer P. T. B., Blakely K. A., Janney M. A., (1987), Production of fine, high-purity, beta SiC powder, *Advances in Ceramics*, 21, *Ceramic Powder Science*, ed. G. L. Messing, K. S. Mazdiyasni, J. W. Mazdiyasni and R. A. Haber. The American Ceramic Society, Westerville, OH, pp: 257-263.

Semmelroth K., Schulze N., Pensl G. , Growth of SiC polytypes by the physical vapour transport technique, *Journal of Physics: Condensed Matter*, 16, (2004), pp: S1597-S1610.

Schwetk K. A., Werheit H., Nold E., (2003), Sintered and monocrystalline black and green silicon carbide: Chemical compositions and optical properties, *Ceramic Forum International*, 80 (12).

Sharma R., Rao D.V. S., Vankar V.D., (2008), Growth of nanocrystalline β-silicon carbide and nanocrystalline silicon oxide nanoparticles by sol gel technique, *Materials Letters*, 62, pp: 3174-3177.

Shen T. D., Koch C. C., Wang K. Y., Quan M. X., Wang J. T., (1997), Solid-state reaction in nanocrystalline Fe/SiC composites prepared by mechanical alloying, *Journal of Materials Science*, 32, 14, pp: 3835-3839.

a. Stein R.A., lanig P, (1993) Control of polytype formation by surface energy effects during the growth of SiC monocrystals by the sublimation method, *Journal of Crystal Growth,* 131, pp: 71-74.

b. Stein R.A., Lanig P., Leibenzeder S., (1992), Influence of surface energy on the growth of 6H- and 4H-SiC polytypes by sublimation, *Materials Science and Engeneering* B,11, pp: 69-71.

Straubinger T.L., Bickermann M., Weingaertner R., Wellmann P.J., Winnacker A., Aluminum p-type doping of silicon carbide crystals using a modified physical vapor transport growth method, *Journal of Crystal Growth*, 240, (2002), pp: 117-123.

Suryanarayana C., (2001), Mechanical alloying and milling, *Progress in Materials Science,* 46, pp: 1-184.

Tachibana T., Kong H.S., Wang Y.C, Davis R.F., (1990), Hall measurements as a function of temperature on monocrystalline SiC thin films, *Journal of Applied Physics*, 67, pp: 6375-6381.

Tairov M Yu., Tsvetkov V. F., (1978), Investigation of growth processes of ingots of silicon carbide single crystals, *Journal of Crystal Growth*, 43, pp: 209-212.

Tham M. L., Gupta M., Cheng L., (2001), Effect of limited matrix-reinforcement interfacial reaction on enhancing the mechanical properties of aluminium-silicon carbide composites, *Acta Materiala*, 49, pp: 3243-3253.

Vadakov Y.A., Mokhov E.N, M.G. Ramm, A.D. Roenkov, (1992), Amorphous and crystalline silicon carbide III, in: Harris G.L., Spencer M.G., C.Y.- W. Yang (Eds.), Springer, New York, , p. 329.

Wang G., Krstic V., (2003), Effect of Y_2O_3 and total oxide addition on mechanical properties of pressureless sintered β-SiC, *Journal of Materials Science and Technolology*, 19(3), pp: 193-196

Wellmann P., Desperrier P., Müller R., Straubinger T., Winnack A., Baillet F., Blanquet E., Dedulle J.M., Pons M., SiC single crystal growth by a modified physical vapor transport technique, *Journal of Crystal Growth,* 275, (2005), pp: e555-e560.

White A. D., Oleff M. S., Boyer D. R., Budinger A. P., Fox R. J., (1987), Preparation of silicon carbide from organosilicon gels: I. Synthesis and characterization of precursor gels. *Advanced Ceramic Materials,* 2(l), pp: 45-52.

White A. D., Oleff M. S., Boyer D. R., Budinger A. P., Fox R. J., (1987), Preparation of silicon carbide from organosilicon gels: II. Gel pyrolysis and SiC characterization. *Advanced Ceramic Material,* 2(l), pp: 53-59.

Ye LL, Quan MX. (1995), Synthesis of nanocrystalline TiC powders by mechanical alloying, *Nanostructured Materials*,5, 1, pp :25-31.

Zhang B., Li J., Sun J., Zhang S., Zhai H., Du Z., (2002), Nanometer silicon carbide powder synthesis and its dielectric behavior in the GHz range, *Journal of the European Ceramic Society*, 22, pp: 93-99.

Zhao D.L., Luo F., Zhou W.C., (2010), Microwave absorbing property and complex permittivity of nano SiC particles doped with nitrogen, *Journal of Alloys and Compounds*, 490, pp: 190–194.

Zhao D., Zhao H., Zhou W., (2001), Dielectric properties of nano Si/C/N composite powder and nano SiC powder at high frequencies, *Physica E*, 9, pp: 679-685.

Zou G., Cao M., Lin H., Jin H., Kang Y., Chen Y., (2006), Nickel layer deposition on SiC nanoparticles by simple electroless plating and its dielectric behaviours, *Powder Technology*, 168, 2, pp:84-88.

Zheng Yo., Zheng Yi., Lin L. X., Ni J., Wei K. M., (2006), Synthesis of a novel mesoporous silicon carbide with a thorn-ball-like shape, *Scripta Materialia*, 55, pp: 883–886.

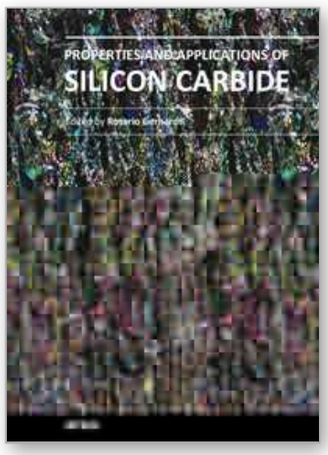

Properties and Applications of Silicon Carbide

Edited by Prof. Rosario Gerhardt

ISBN 978-953-307-201-2
Hard cover, 536 pages
Publisher InTech
Published online 04, April, 2011
Published in print edition April, 2011

In this book, we explore an eclectic mix of articles that highlight some new potential applications of SiC and different ways to achieve specific properties. Some articles describe well-established processing methods, while others highlight phase equilibria or machining methods. A resurgence of interest in the structural arena is evident, while new ways to utilize the interesting electromagnetic properties of SiC continue to increase.

How to reference

In order to correctly reference this scholarly work, feel free to copy and paste the following:

Houyem Abderrazak and Emna Selmane Bel Hadj Hmida (2011). Silicon Carbide: Synthesis and Properties, Properties and Applications of Silicon Carbide, Prof. Rosario Gerhardt (Ed.), ISBN: 978-953-307-201-2, InTech, Available from: http://www.intechopen.com/books/properties-and-applications-of-silicon-carbide/silicon-carbide-synthesis-and-properties

INTECH
open science | open minds

InTech Europe
University Campus STeP Ri
Slavka Krautzeka 83/A
51000 Rijeka, Croatia
Phone: +385 (51) 770 447
Fax: +385 (51) 686 166
www.intechopen.com

InTech China
Unit 405, Office Block, Hotel Equatorial Shanghai
No.65, Yan An Road (West), Shanghai, 200040, China
中国上海市延安西路65号上海国际贵都大饭店办公楼405单元
Phone: +86-21-62489820
Fax: +86-21-62489821

IntechOpen